# Alma Mater Studiorum Università di Bologna
# Archivio istituzionale della ricerca

Outlining the mission profile of agricultural tractors through CAN-BUS data analytics

(Article begins on next page)

10 February 2025

# OUTLINING THE MISSION PROFILE OF AGRICULTURAL TRACTORS THROUGH CAN-BUS DATA ANALYTICS

1  Michele Mattetti[a*], Mirko Maraldi[a], Nicola Lenzini[b], Stefano Fiorati[b], Eugenio Sereni[c],
2  Giovanni Molari[a]
3  [a] Department of Agricultural and Food Sciences, Alma Mater Studiorum – University of Bologna, viale G.
4  Fanin, 50, 40127, Bologna, Italy
5  [b] CNH Industrial – Tractor Innovation Engineering, viale delle Nazioni 55, 41100, Modena, Italy
6  [c], viale delle Nazioni 55, 41100, Modena, Italy
7  [*] tel. +39 051 2096174, fax +39 051 2096178, email: *michele.mattetti@unibo.it*
8

9  ## Abstract

10  Tractor manufacturers need to know how farmers use their agricultural tractors for an

11  optimal machine design. Tractor usage is not easy to assess due to the large variability of field

12  operations. However, modern tractors embed sensors integrated into the CAN-BUS network

13  and their data is accessible through the ISO 11783 protocol. Even though this technology has

14  been available for a long time, the use of CAN-BUS data for outlining the tractor usage is still

15  limited, because a proper post-processing method is lacking. This study aimed to present a novel

16  classification scheme of CAN-BUS data which permits to outline the tractor usage. On a tractor,

17  a CAN-BUS data logger and a GNSS receiver were installed, and real-world data were recorded

18  for 579 hours. Thus, data was obtained in the most realistic condition. Tractor positions were

19  classified using GIS layers while operating conditions were classified depending on the usage

20  of the tractor's subsystems. The method highlights that showed to be able to detect the 97% of

21  the logged data and that the tractor operated on the field in working, on idle, and moving duties

22  for 65%, 18% and 16% of the time, respectively. The method allows a far more precise outline

23  of tractor usage opening opportunities to obtain large benefits from massively collected CAN-

24  BUS data.

25

| Table 1: Nomenclature | | |
|---|---|---|
| $D_{OFF}$ | Distance travelled in out-of-work state | [m] |
| $D_{ON}$ | Distance travelled in in-work state | [m] |
| $GNSS$ | Global navigation satellite system | [−] |
| $n_e$ | Engine speed | [rpm] |
| $n_{PTO,f}$ | front PTO speed | [rpm] |
| $n_{PTO,r}$ | rear PTO speed | [rpm] |
| $P_e$ | Engine power | [$kW$] |
| $RWI$ | Rear hitch in work indication | [−] |
| $T_e$ | Actual engine-percent torque | [%] |
| $T_f$ | Nominal friction-percent torque | [%] |
| $T_H$ | Headland turns duration | [s] |
| $T_r$ | Engine reference torque | [Nm] |
| $V_t$ | Tractor ground speed | [$km\ h^{-1}$] |

27

## Introduction

29    The typical usage of a tractor model is described through its mission profile, which is a

30    synthetic description of a tractor use. Mission profiles report the factors that influence the

31    operational durability of tractor components (Johannesson & Speckert, 2013). A mission profile

32    may report:

33    • the typical tractor service life;

34    • the typical contribution of each operating modes on the service life (e.g. ploughing, on-

35     road, and off-road transportations, etc);

36    • how each component is typically used (e.g. the input power and speed on gearboxes,

37     vehicle ground speed, etc).

38

39    Mission profiles are essential for a proper design/selection of tractor components (Sehab et

40    al., 2011) or for designing durable and reliable machines with an optimal balance between

41    under-designs and over-designs (Plaskitt & Musiol, 2002).

42    Mission profiles of agricultural tractors include several factors, and these factors make their

43    mission profile estimations much more challenging than that of road vehicles. Indeed, a road

44    vehicle may travel on only three different types of roads (e.g. highway, city, country road) and

45    two types of load levels (the driver alone and with 4 passengers and luggage) (Marchesani et

46    al., 1992); on the other hand, row crop tractors may be used for a larger variety of uses (e.g.

47    road transportation, soil preparation, sowing, haying, etc.), and each can be accomplished at

48    different load levels due to the different ground conditions.

49    To estimate a mission profile, tractor usage from a sample of farmers is necessary. This is

50    typically carried out through surveys aimed at obtaining information about the farm size, yearly

51    usage of tractors, list of farming operations carried out in the farm, and how each operation is

52    performed (Mattetti et al., 2012). This approach is usually adopted for its easiness in obtaining

53    data from large samples, but the obtained information is biased toward subjective judgements,

54    which could lead to unreliable mission profiles. A different approach consists in installing

55    switchboards inside tractor cabs (Paraforos et al., 2017) or through specific smartphone apps

56    (e.g. 365Farmnet) which allow farmers to assign the task they are accomplishing with the

57    tractor. However, these approaches require a manual effort of farmers, who may forget the task

58    assignment.

59    In modern tractors, the operating parameters of all the tractor subsystems can be monitored

60    using CAN-BUS technologies together with SAE J1939, and ISO 11783 protocols (ISO, 2012;

61    Molari et al., 2013; SAE, 2006). In previous studies, CAN-BUS messages were successfully

62    used to outline the usage of specific tractor components (Mattetti et al., 2019), to determine

63    field efficiencies of agricultural machinery (Pitla et al., 2014, 2016) or to monitor specific

64    tractor operating modes (Molari et al., 2019). The best approach for a proper mission profiling

65    would be recording and analysing real-world CAN-BUS data of a large fleet of tractors. In this

66    way, the recording process would not interfere with farming activities and data would be

67  recorded in the most realistic conditions. But then, the environment where vehicles operate is

68  unknown, and advanced classification approaches are essential for a reliable estimation of the

69  mission profile (Fugiglando et al., 2019). Data classification is the process of grouping together

70  portions of signals related to the same work state (Zhang et al., 2017). A sort of data

71  classification is already provided by telemetric data service supplied by each tractor

72  manufacturer (New Holland MyPLM Connect, John Deere JDLink). In these tools, the work

73  states are defined on the basis of simple threshold-rules, in other words a work state is defined

74  when any signal exceeds a threshold. For example, in telemetric data services, tractors are:

75  • on fieldwork state when the three-point linkage is down, but farmers may drive bare

76  tractors on the field with the three-point linkage in the down position.

77  • on moving state when its speed exceeds a threshold specified by the driver (i.e.

78  25 km h$^{-1}$), but the proper value may change in function of the road state (i.e. presence

79  of speed humps, road damages, etc).

80  For these reasons, this approach is far too simplistic and data misclassifications are not

81  infrequent. More advanced rule-based algorithms were proposed for specific tractor operations

82  (Ettl et al., 2018), and forage harvesters (Harmon et al., 2018; Zhang et al., 2017). Rule-based

83  algorithms require knowledge from the experts and a reasonable amount of effort to design and

84  implement effective rules for real-world data. Indeed, in real-world conditions, tractor

85  operativity may change according to a variety of operating conditions (in terms of soil,

86  implement type, driving style). Thus, for outlining the tractor usage, a robust and flexible

87  method must be developed, which can deal with the variability induced by the variability of

88  tractor manoeuvres (Mattetti, Molari, et al., 2017).

89  This article aimed to develop a robust and automatic classification scheme able to identify

90  the tractor mission profile using real-world CAN-BUS, and trajectory data.

## Materials and methods

91

92 *Data acquisition*

93    The analysis was applied to a New Holland T7 tractor (CNH Industrial N.V., Amsterdam,

94 NL) whose specifications are reported in Table 2. This was chosen because tractors of this class

95 are rich in terms of embedded sensors allowing for comprehensive monitoring of the activity

96 of the different embedded subsystems.

| Table 2 – Specifications of the tractor used in this study. | | |
|---|---|---|
| Maximum engine power | $(kW)$ | 198 |
| Engine displacement | $(m^3)$ | 6.728 |
| Number of cylinders | $(-)$ | 6 |
| Engine tier | $(-)$ | 4B |
| Transmission | $(-)$ | Continuously variable transmission |
| Number of auxiliary hydraulic valves | $(-)$ | 4 |
| Three-point linkage | $(-)$ | Rear |
| PTO | $(-)$ | Front and rear |

97

98    The tractor was in use between the June 2018 and October 2019 by 5 professional drivers

99 with more than twenty years of experience. The tractor was used in the Agricultural Farm of

100 the University of Bologna. The size of the farm is 500 ha, where 67%, 10% and 23% of the

101 land are devoted to cereals, orchards, and haying, respectively. The farm is distributed in three

102 different units (i.e. areas where tractors are stored overnight) located in three different towns;

103 the farther locations are 35 km apart. In this farm, this tractor is mostly used for transportation

104 tasks and primary and secondary tillage tasks.

105    A stand-alone CAN-BUS data-logger optimised by CNH Industrial was installed on the

106 tractor. The data-logger was set up to automatically record all the CAN-BUS messages anytime

107 the tractor engine was turned on so that the recording process did not interfere with farming

108 activities. In particular, the CAN-BUS data logger is equipped of two separated CAN-BUS

109 channels compatible with the standards: SAE J1939-14 (SAE, 2016a) and SAE J1939-15 (SAE,

110   2018b). The data-logger embeds a BLE (Bluetooth low energy) scanner which scans the BLE

111   beacons in its surroundings (up to 10 meters) every second. Commercial BLE beacons

112   (Mokosmart M1 Beacon, Shenzen, China) were attached to the implements available at the

113   farm as suggested in other studies (Calcante & Mazzetto, 2014) (Fig. 1).



114
115   *Fig. 1: A trailer used during the project. Enclosed in the yellow circle, a BLE beacon that permitted the*
116   *identification of the trailer.*

117   The BLE scanner records the identifiers of the detected BLE beacons to record implement

118   connected to the tractor. Moreover, a Garmin Dash Cam 55 (Garmin Ltd., Olathe, KS, USA)

119   was installed on the windshield of the tractor to document the tractor activity in order to ensure

120   the reliability of the classification scheme.

121   For the purpose of this study, only signals with the following Suspect Parameter Numbers

122   (SPNs) and Parameter Group Numbers (PGNs) (ISO, 2012; SAE, 2013) were used for the

123   analysis:

124   • SPN 544 and PGN 65251: "*Engine Reference Torque*" that reports the torque as a

125      percent of Engine Reference Torque (SPN 544 and PGN 65251) and it is denoted as $T_r$

126      in the following.

127 • SPN 513 and PGN 61444: "*Actual Engine - Percent Torque*" that reports the torque as a

128 percent of $T_r$ , and it is denoted as $T_e$ in the following.

129 • SPN 513 and PGN 5398: "*Nominal friction-percent torque*" that reports the frictional

130 and thermodynamic loss of the engine itself, pumping torque loss and the losses of fuel,

131 oil and cooling pumps as a percent of $T_r$, and it is denoted as $T_f$ in the following.

132 • SPN 190 and PGN 61444: "*Engine Speed*" that reports the revolution speed of the engine

133 crankshaft, and it is denoted as $n_e$ in the following.

134 • SPN 1883 and PGN 65090: "*Rear PTO output shaft speed*", that reports the speed of the

135 rear PTO.

136 • SPN 1882 and PGN 65090: "*Front PTO output shaft speed*" that reports the speed of the

137 front PTO.

138 • SPN 1877 and PGN 65093: "Rear hitch in-work indication " that reports the rear hitch

139 is positioned below (in-work) or above (out-of-work) 85% of the position of the rear

140 three-point linkage (SPN 1873 and PGN 65093). This signal is denoted as $RWI$ in the

141 following.

142 Moreover, a GNSS (global navigation satellite system) receiver with an update rate of 10

143 Hz, with no differential correction, and with a claimed accuracy of 2.5 m (in terms of circular

144 error probable) (IPESpeed, IPETronik GmbH, Baden Baden, Germany) was installed in the

145 tractor to monitor its position and its tractor ground speed ($V_t$).

146 *Data analysis*

147 All the signals were interpolated at 10 Hz using a cubic spline so that the sampling rate of

148 all the signals was the same. From the recorded data, the delivered engine power ($P_e$) was

149 calculated as follows:

150
$$P_e = T_r \cdot \frac{T_e - T_f}{100} \cdot n_e \frac{2\pi}{60}$$

151   All the portions of the recorded signals acquired when the tractor position was not logged

152   (because the GNSS receiver did not obtain a strong enough satellite signal, e.g. when the tractor

153   was moved out from an indoor environment) were excluded from the analysis. Tractor positions

154   were classified into three categories:

155   • *road*, anytime the position was closer than 3 m to any road stretch. The 3 m

156   threshold was chosen based on the circular error probability of the GNSS receiver

157   used in this study. For a full automation of the process, this was carried out by

158   checking if there is any intersection point between any road stretch and a circle, with

159   a radius of 3m, centred in the tractor position.

160   • *field*, anytime the position was inside the boundary of any field plot.

161   • *farm*, anytime the position was inside the boundary of any farm unit.

162   For the classification of the tractor position, a shapefile containing the road network, the

163   boundaries of field plots, and the boundaries of the farm units were created. The creation of the

164   shapefile started by downloading the soil use and the road network from the geoportal of the

165   Emilia Romagna region (*Dati preconfezionati — GeoER*, 2019). To this shapefile, the

166   boundaries of three farm units were added.

167   The tractor operating conditions were classified into three categories: idling, moving, and

168   three-point linkage use. Idling condition was defined as the state where the tractor was standing

169   with no use of any PTO for more than 5 s; the duration threshold was added in order to not

170   include portions where the tractor was temporary still during manoeuvring, like reversing the

171   tractor direction at the headlands. *Moving* condition was defined as the state where tractor

172   ground speed was greater than 0 km h$^{-1}$ with no use of the three-point linkage or both PTOs.

173   *Three-point linkage use* was defined as the state where the three-point linkage was used for

174   field operations. This occurs anytime a sequence of a pass, headland, and pass was repeated.

175   *RWI* signal shows a rectangular waveform, but when the tractor operates on field operations,

176 repetitive pulses could be observed (Fig. 2 - right). A method for discerning field operations

177 from implement hitching or machine moving activities was developed and it is described in the

178 following.

179
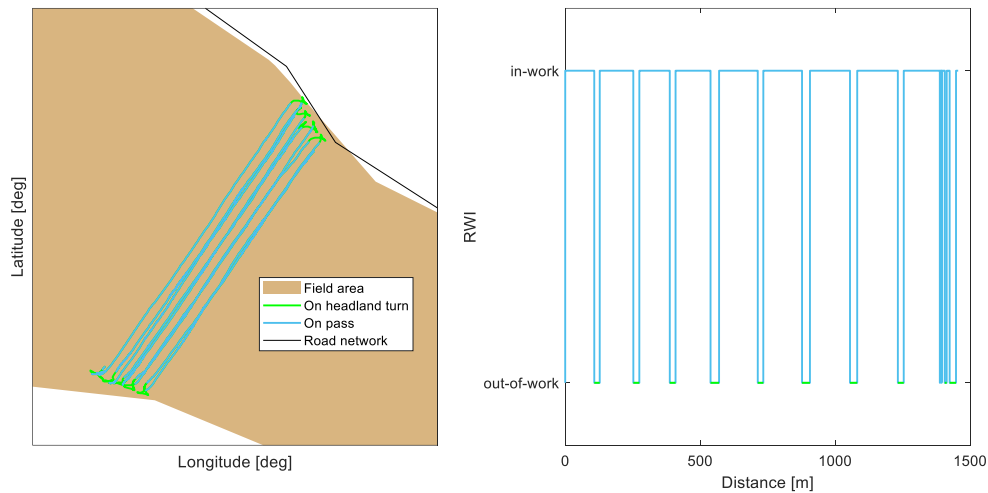


180
181 *Fig. 2: Tractor trajectory (on left), and RWI signal (on right) during a field operation with a plough.*

182 First, the distance travelled by the tractor on each in-work ($D_{ON}$) and on the out-of-work ($D_{OFF}$)

183 states of *RWI* signal was calculated. For field operations, $D_{ON}$ and $D_{OFF}$ represent the length of

184 passes and headlands, respectively. Both depend on several operating parameters like length of

185 fields, and headland strategy (Paraforos et al., 2018). For field operations, $D_{OFF}$ was usually

186 included in a range between 1 and 70 m. Values of $D_{OFF}$ below the lower bound occurred on

187 implement hitching and values of $D_{OFF}$ above the upper bound occur when the tractor switched

188 from or to a moving operation. The above range was determined using the following approach:

189    • Identification of the portions where the tractor was operating in the field from video

190      data collected with the camera.

191    • Extraction of all the logged signals in this portion.

192    • Calculation of histograms of $D_{on}$ data of 1200 headlands and from it the threshold

193      was set.

194    The algorithm started by calculating the series of $D_{ON}$ and $D_{OFF}$, and *three-point linkage use*

195    classification occurred in the timespan where $D_{OFF}$ are included in the beforementioned range.

196    When this classification occurs, the high levels of $RWI$ described the passes, while the low

197    levels of $RWI$ described the headlands. Then, the headland duration was calculated as the time

198    elapsed between the falling and rising edge of $RWI$ signal when the tractor was in *three-point*

199    *linkage usage*.

200       The work states were defined based on a combination of the classification of the tractor

201    position and the tractor operating activity (Table 3).

| *Table 3 – Rule used for the work states which characterise the tractor use.* | | | |
|---|---|---|---|
| ***Work states*** | ***Classified tractor position*** | ***Boolean operation*** | ***Classified tractor operating activity*** |
| *On-road moving* | *Road* | *AND* | *Moving* |
| *Off-road moving* | *NOT(Road)* | *AND* | *Moving* |
| *Field work* | *Field* | *AND* | *three-point linkage use* |
| *Idle@field* | *NOT(Road)* | *AND* | *Idle* |
| *Idle@farm* | *Farm* | *AND* | *Idle* |
| *Marginal* | *Otherwise* | | |

202

203       The idling on road was included into *marginal* because its contribution is of minor

204    importance to the entire idling (Molari et al., 2019).

205       An example of the classification of the work states is reported in Fig. 3. One can note that

206    in the first portion (in the first 6 min of the time histories) the tractor was classified as on-road

207    moving task; indeed, the tractor was running at around 40 km h$^{-1}$ and $P_e$ was on average low

208    with peaks when high tractor accelerations occurred. On the other hand, the last portion (from

209    13 min) was classified as field work, indeed $V_t$ was lower than 10 km h$^{-1}$ and $P_e$ is close to

210    engine limit.
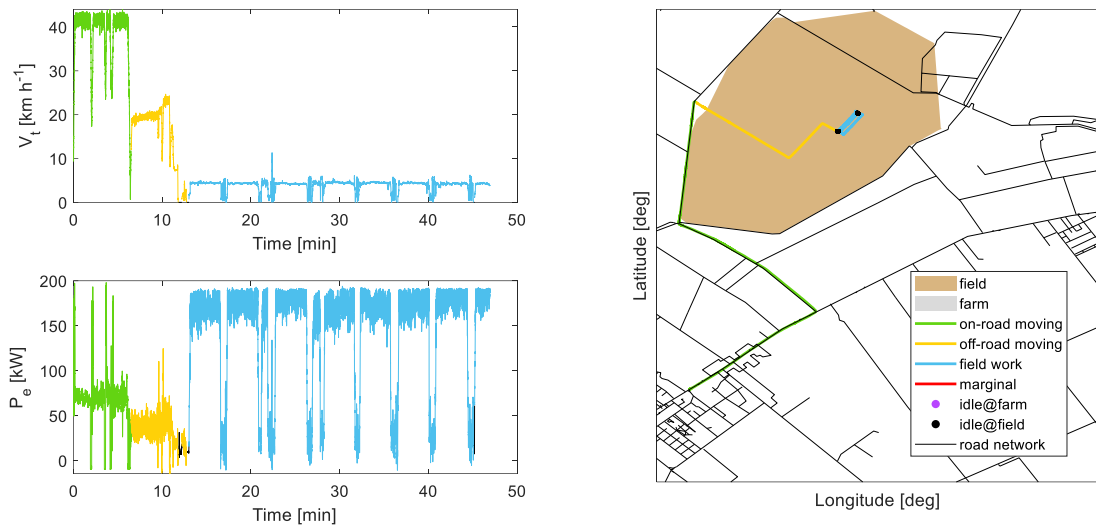
*Fig. 3: Classification example of tractor ground speed (on the top left) and engine power (on the bottom left) compared with the tractor trajectory data (on right).*

213     In this article, a task was defined as the portions where neither work states nor hitched

214     implement was changed. For each task, the average values of all signals were calculated; for

215     the subsequent dataset, outliers (i.e. misclassifications) were identified through the confidence

216     ellipse method. This method consists of computing the confidence ellipse between two

217     variables and considering outliers data points falling outside the confidence ellipse (Hodge &

218     Austin, 2004). For drawn implements, the two variables were $V_T$ and $P_e$ (Fig. 4); as the power

219     demand of this type of implements is mostly dependent on the working speed (Mattetti, Varani,

220     et al., 2017), while for PTO-driven implements, the two variables were $n_{PTO,*}$ (* stands for $f$

221     for front mounted implements and $r$ for rear mounted implements) and $P_e$, as the power demand

222     of this type of implements is dependent on the speed of the PTO (Balsari et al., 2020). The

223     confidence level was set at 90%. A multivariate approach was necessary, since a low demanding

224     ploughing may not be an outlier if the ground speed is low as well.
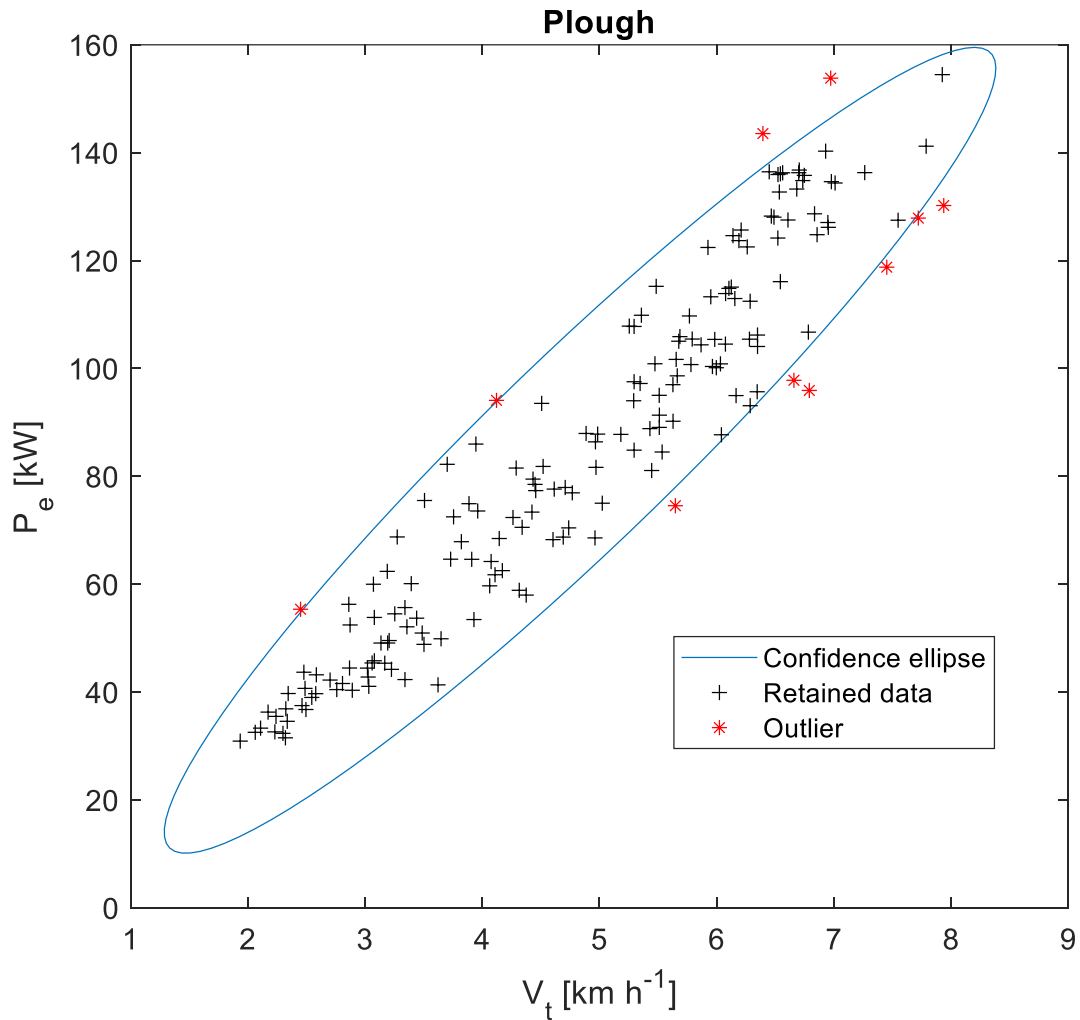
*Fig. 4: An example of the outlier detection method for the field work tasks with plough. Only passes were considered.*

## Results and Discussion

The tractor was used for 107 days amounting to 579 hours overall. The tractor was used with 11 implements, but 5 of them were used for 84% of the time (Fig. 5). For 78% of the time, the tractor was used for plough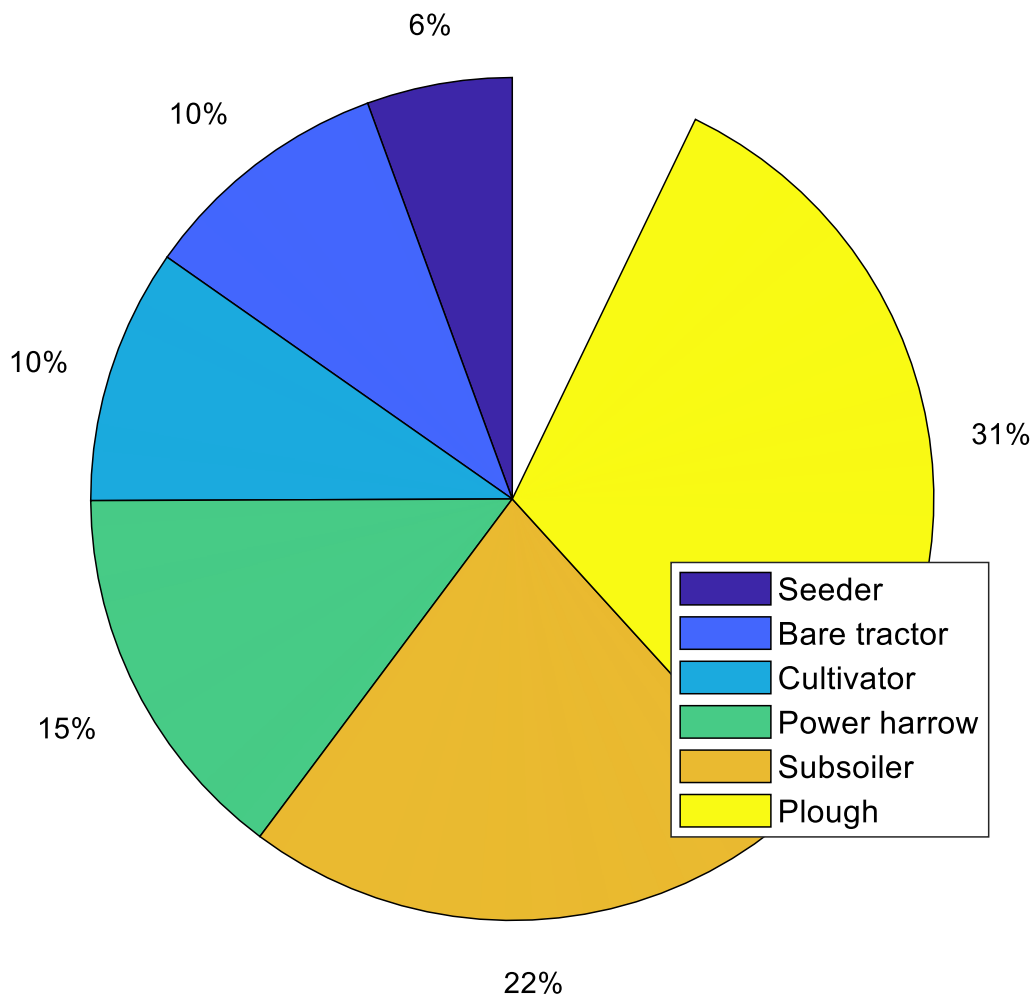ing, subsoiling, harrowing, and cultivating. Thus, the analysis was focused on the data related to those operations for the larger amount of available data. The tractor was used with no implement for 10% of the time, and in this configuration, the tractor was mostly moved from a farm unit to another.

*Fig. 5: Pie chart reporting the contribution of each implement on the operating time. In the chart, the implements used for less than 20 hours were not plotted for sake of clarity.*

The tractor was used for field work tasks for 65% of the time and 18% of the time for idling activities (Fig. 6). The amount of idling is below the average value reported in the study by Perozzi et al. (2016) where the idling of a large sample of tractors was analysed.
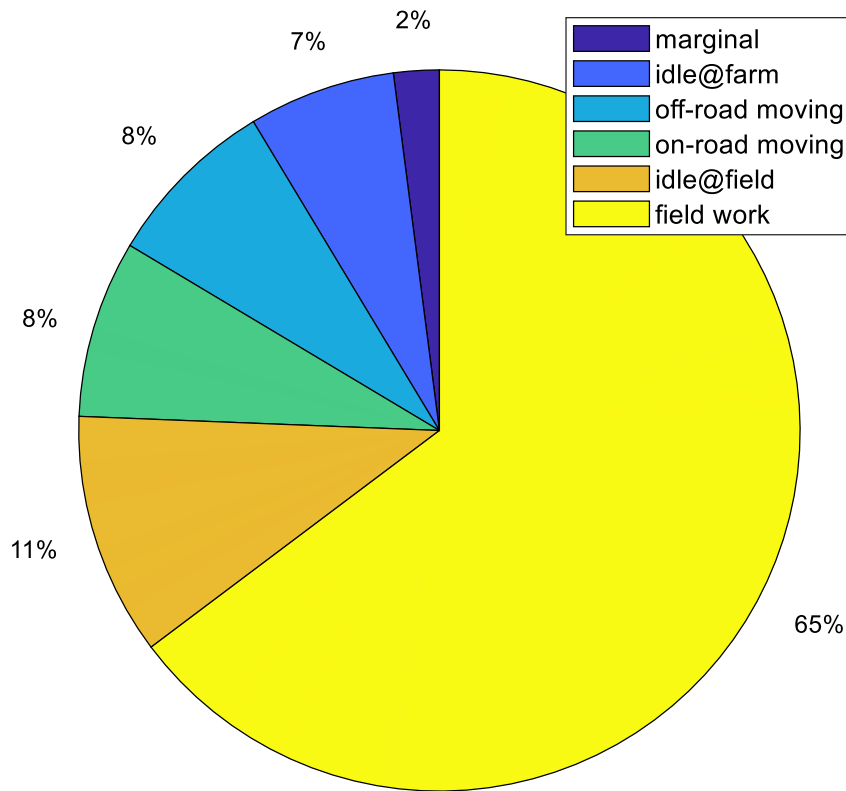
The time contribution of *off-road moving* state is lower than that of the *on-roading moving* state. This is because the farm where the tractor was used is spread over a large area, which leads to infrequent but prolonged *on-road moving* states. Indeed, for *off-road moving* work state, the number of tasks are 38% of all the identified tasks and their average duration is 172 s. On the other hand, for *on-road moving* work states, the number of tasks are and 11% of all the identified tasks and their average duration is 478 s, respectively. The time contribution of *idle@field* work state is larger than that of *idle@farm* because the amount of idling stops on the field is much more frequent than those at the farm due to the varied source of stops, such as rest stops, driver turnover, checking the performance, removal of crop residual on implements (Hunt & Wilson, 2015). On the other hand, *idle@farm* state mostly occurs at the beginning and the end of the workday, and mostly for machine servicing or adjustment, implement hitching and machine parking (Molari et al., 2019). The sum of the time contributions for the *idle@field* and

255  *field work* states provide an insight of the portion of time where the tractor operated for field

256  related activities, and it includes the time for actual work, headlands, field setting, and

257  maintenance at field (Lovarelli et al., 2017). Headlands contribute to 24% of the entire *field*

258  *work* state and this figure is aligned to that of Ettl et al. (2018). Moreover, the time contribution

259  of the *marginal* is less than 3%, which means that the defined work states can describe most of

260  the tractor operations. In Fig. 7, the relative frequency of headland durations ($T_H$) for 10065

261  headlands is reported. $T_H$ range from 3 s up to 230 s and it is strongly dependent on the headland

262  patterns. 50% of the headlands ranged from 20 and 40 s and this result is aligned with that

263  reported in other studies (Ettl et al., 2018; Paraforos et al., 2018).
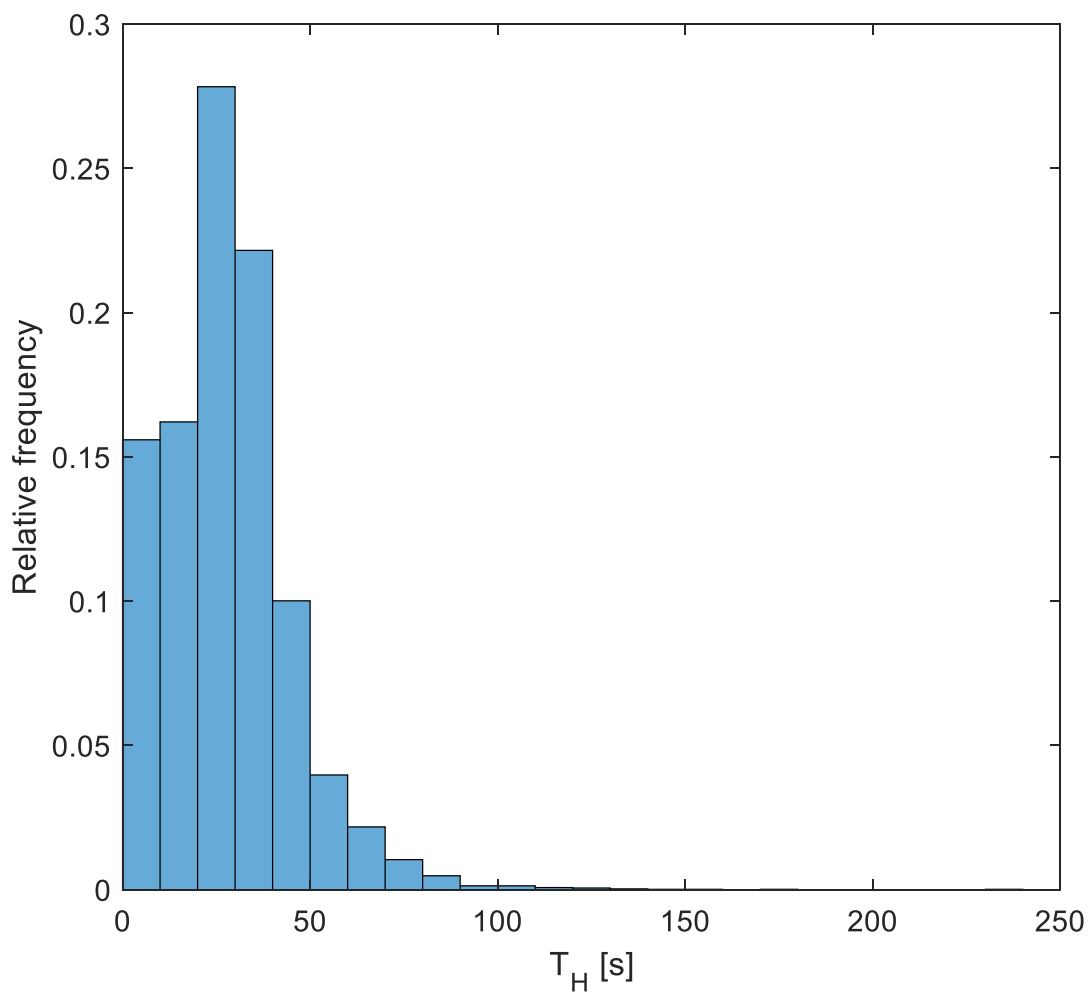


264
265  *Fig. 7: Relative frequency distribution of the duration of the identified headlands.*

266    Headlands shorter than 20 s are not infrequent, and they account for 32% of the headlands.

267    These occur when the tractor worked around the field border where the circuitous turn strips at

268    corner diagonals working pattern is adopted (Hunt & Wilson, 2015). In the most extreme cases,

269    $T_H$ is lower than 10 s, this occurs for an unconventional type of headland pattern. In particular,

270    the farmer tilled two different fields separated by a country road and no turns can be observed

271    in the tractor trajectory (Fig. 8). In the same plot, also headlands longer than 100 s can be

272    observed, which occurred because the overlapping alternation pattern was adopted.
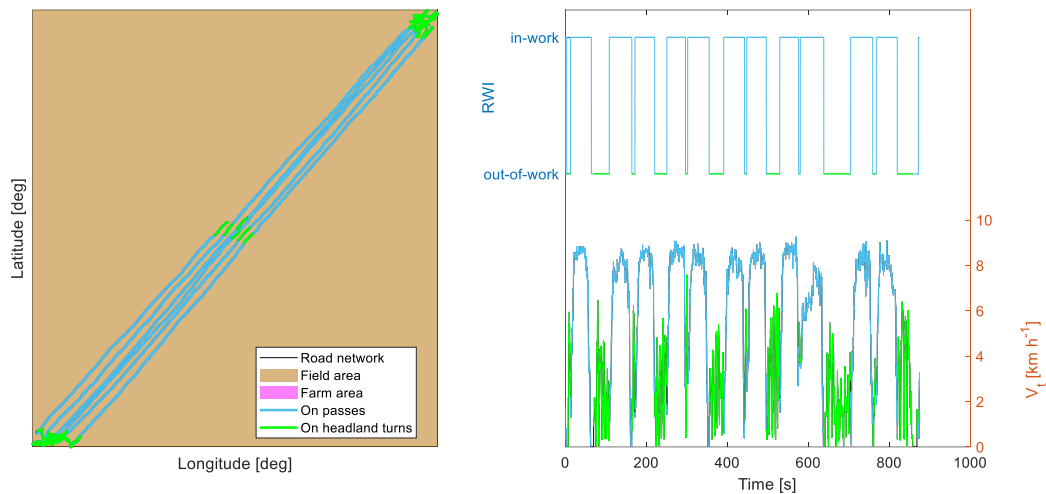


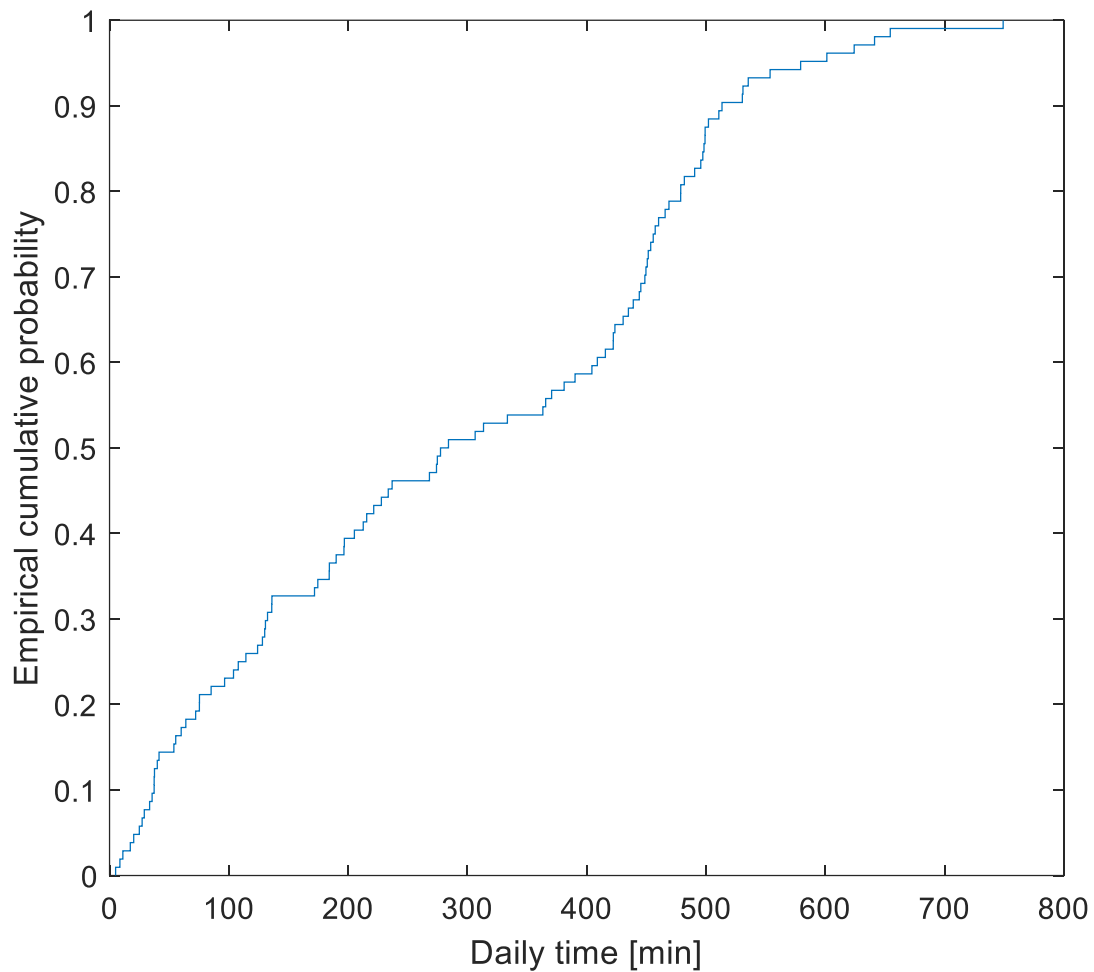273
274                          *Fig. 8: Headland pattern where $T_H$ was lower than 10 s and longer than 100 s.*

275    The daily usage of the tractor ranges from 20 min to up 750 min; and the 50% of the days

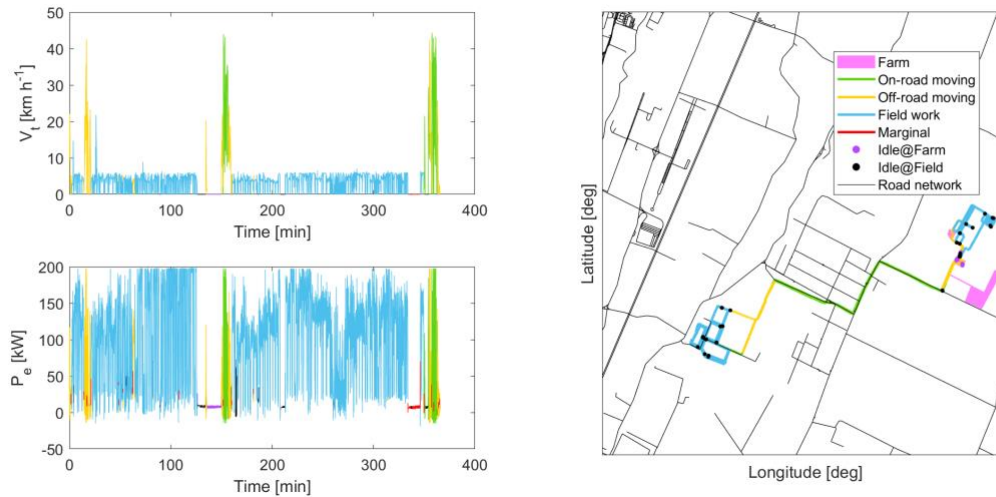276    the tractor was used for more than 280 min (Fig. 9).

277

280    In Fig. 10, a typical daily operating cycle of the tractor is reported. This is composed of the

281    following activities:

282        1.  tractor idling at the farm at the beginning of the day for implement hitching or,

283            machine servicing and then moving the tractor from any farm unit to the field;

284        2.  field work where idling stops may occur for field machine maintenance;

285        3.  moving the tractor from the field to any farm unit.

286    When the driver turnover did not occur on field, or when changes in the tractor field

287    operation occurred during the day. The afore-described cycle was repeated twice in a day since

288    the driver went back to any farm unit for lunch or implement swapping.
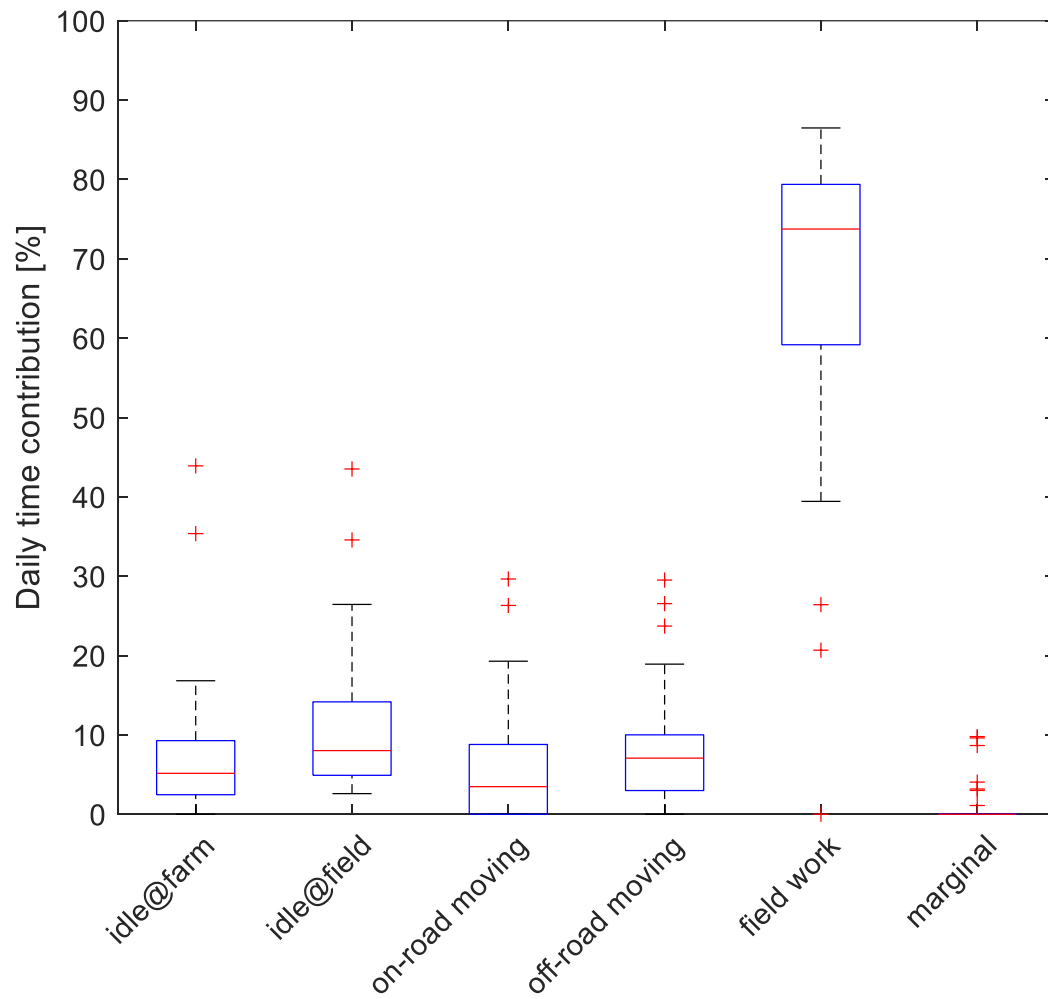
In Fig. 11, the daily time contribution of the different tractor work states is reported. The largest contribution is provided by the *field work* state for 50% of the days, and it contributed to 73% of the entire daily activity. The other work states contribute less than 30% (without considering the outliers). The tractor was not used for field activities for 4 days since the daily time contribution of the *field work* state is 0%. In those days, larger contributions of the idling and moving states can be observed and the tractor was used for off-field activities because the weather conditions did not permit any field activities. Those activities consisted of machine servicing or moving implements from a farm unit to another. The results reported in other studies are aligned to the median values of the daily time contribution calculated in this study (Ettl et al., 2018; Kortenbruck et al., 2017).

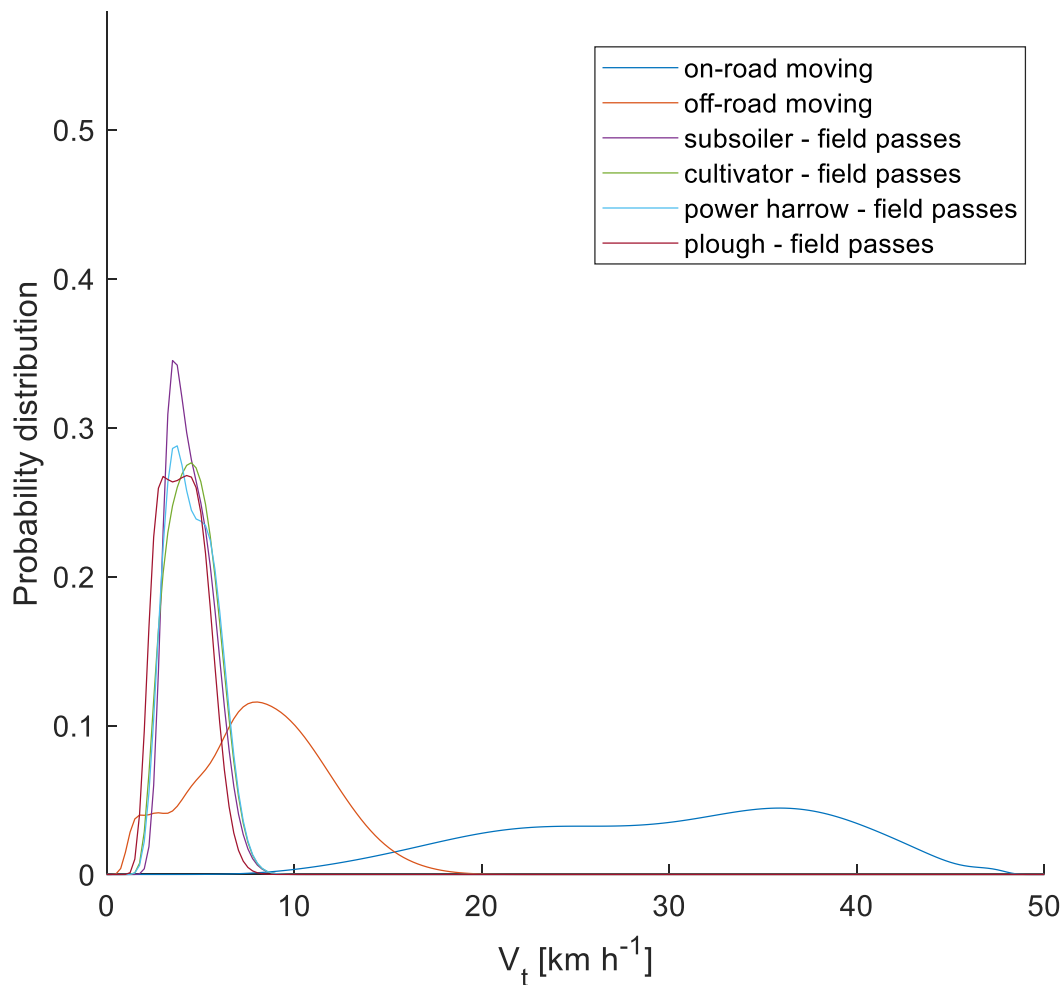305    The kernel smoothed probability distributions of $V_t$ of the two moving states, and field work

306    states with the four most frequent implements are reported in Fig. 12. All the distributions have

307    unique modes except for that of the plough.

308

309

Fig. 12: Kernel smoothing distribution of tractor operating speed at various work states. Headlands were not considered on field operations.

In order to compare the distributions obtained in this study with those reported in the ASAE D497.7 (2011), the 10th and 90th percentiles, and the modes are reported in Table 4.

| Table 4 – Main statistics of the speed distributions | | | |
|---|---|---|---|
| **Tractor states** | **10th percentile [km h-1]** | **Mode [km h-1]** | **90th percentile [km h-1]** |
| on-road moving | 20.0 | 36.0 | 40.0 |
| off-road moving | 3.5 | 8.0 | 12.4 |
| subsoiler - field passes | 3.3 | 3.5 | 5.8 |
| cultivator - field passes | 3.0 | 4.2 | 6.0 |
| power harrow - field passes | 3.2 | 3.7 | 5.9 |
| plough - field passes | 2.6 | 3.0 / 4.2 | 5.5 |

316     The speed values observed in this study are slightly lower than those reported in the ASAE

317     standard. For example, according to the ASAE standard, the speed range of a mouldboard

318     plough is between 5 and 10 km h$^{-1}$, whereas it was found to be between 2.6 km h-$^1$ and 5.8 km

319     h$^{-1}$ in this study. This difference may be because data in the ASAE standard is based on data

320     collected in the US, where tractors and fields larger than those available in the farm used in this

321     study.

322         The *off-road moving* distribution is overlapped with the distributions of the *field work* states

323     for $V_t$ lower than 8 km h$^{-1}$ (which corresponds to the 48th percentile of its cumulative

324     distribution), and it is overlapped with the distribution of *on-road moving* state for $V_t$ higher

325     than 12 km h$^{-1}$ (which corresponds to the 85th percentile of its cumulative distribution). This

326     highlights that discerning the moving states only using a threshold-rule for the speed, as it is

327     usually done with many commercial telemetric data services, may lead to misclassifications.

328         In Fig. 13, the confidence level ellipses reported for three work states demonstrate that to

329     fully discern the work states, a multivariate approach is necessary. The ellipses are clearly

330     separated with only minor overlaps occurring between the ellipses of both moving work states,

331     and between the ellipses of *field work* and *off-road moving* work states. $V_t$ is strictly related to

332     $P_e$ depending on the type of the work state. Indeed, on *field work* tasks, the tractor is usually

333     used with high engine loads, low speed and low gear ratios; while for moving tasks, lower

334     engine loads and longer gear ratios are typically used with, high engine loads are limited to

335     acceleration events only. For both moving tasks, $P_e$ increases with $V_t$, due to the fact that the

336     main resistance forces are the motion resistance which increases with the ground speed (Wong,

337     2001). The variability of $V_t$ and $P_e$ inside each operating condition depends on several factors,

338     including driving style, operating, and environmental conditions. Indeed, $P_e$ ranges from 23 kW

339     up to 143 kW for the field work state on passes. Through a visual inspection of the recorded

340     video, it was observed that the tillage operations carried out at low ground speeds (below 3 km

341 h⁻¹) occurred because the soil was severely covered by crop residuals. In these conditions,

342 farmers preferred to work slowly to avoid that the implement could get clogged with crop

343 residuals, which could force the farmer to stop at headlands for implement clearing.

344
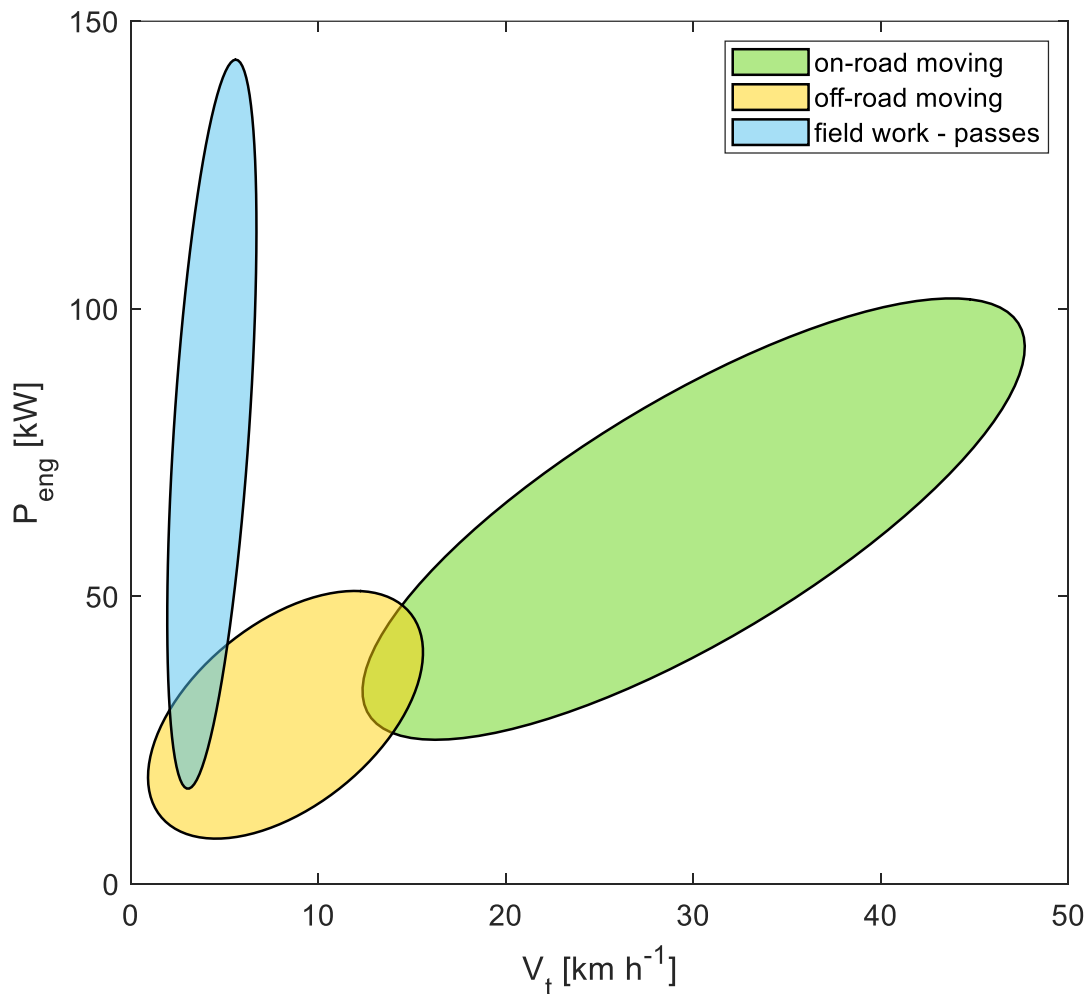


345
346 *Fig. 13: Confidence level ellipses for three non-idling operating states.*

## Discussion

348    Few studies reported algorithms for classifying CAN-BUS data of agricultural tractors, and

349 in all of them, results are based on limited datasets, not collected in real-world conditions. The

350 strength of the classification scheme introduced in this study is the combined use of CAN-BUS,

351 trajectory, and geographical data. This allowed to obtain a finer description of the tractor usage.

352　Indeed, tractor movements were classified based on the road type (i.e. on-road and off-road).

353　On other similar studies, these two operating activities could not be distinguished because the

354　method relies only on CAN-BUS, and trajectory data. Indeed, Kortenbruck et al. (2017)

355　discriminated field from moving activities by evaluating the pattern of the tractor trajectory,

356　which was that of a field operation if parallel traces not further apart than the implement width

357　could be observed. The algorithm is not fully automatic because farmers have to input

358　implement widths, but CEPs of non-RTK- GNSS receivers are of the same order of magnitude

359　of typical implement widths. Thus, field operations cannot be reliably detected only with tractor

360　trajectories. Paraforos et al. (2018) detected headlands and field passes from trajectory data, in

361　particular, headlands were recognized when 180° overturns of tractor heading angle were

362　identified. However, tractors do not always overturns of 180° on headlands especially when

363　tractors work along the field contours (Fig. 8 – left). In Ettl et al. (2018), headland turns were

364　recognised by setting the threshold of the duration with the three-point linkage is fully up

365　position; however, the duration limit is dependent by the headland patterns (Paraforos et al.,

366　2018), and idling stops can be frequent during headlands (Molari et al., 2019) (Fig. 10 – right).

367　　The approach for recognising the field operations adopted in this study is based on the

368　repetitive pattern of the *RWI* signal when tractors operate on field. This approach does not rely

369　on any threshold values of any CAN-BUS parameter, this makes it more effective in dealing

370　with real-world data. Setting the proper thresholds is a critical task because operating

371　parameters may change depending on the type of implement, soil conditions, ground slope, and

372　driving style (i.e. toward productivity or efficiency). The approach used in this paper works

373　only with mounted and semi-mounted implements where a variability on the *RWI* signal can

374　be observed, but the same principle could be used with other signals (e.g. steering angle) where

375　a repetitive pattern could be observed also with trailed implements.

376

## Conclusions

377

378     Information on the usage of agricultural tractors is not well-documented and very often

379     farmers, scientists, and engineers rely on handwritten logbook data. In this paper, a data

380     acquisition system which facilitates the data collection on agricultural tractors, and a novel

381     classification scheme were presented. The novelty of the data acquisition system is that it

382     combines a CAN-BUS logger, a GNSS receiver and a BLE beacon scanner, thus the hitched

383     implement could be recorded even if they are not ISOBUS compliant. Moreover, the novelty

384     of the data analysis method is on the combined use of CAN-BUS, trajectory and geographical

385     data which allowed to introduce a classification scheme more refined than those proposed in

386     similar studies. Indeed, the kinds of tractor activities were classified into 5 states depending on

387     the tractor operating condition and its position. Thanks to the proposed classification scheme,

388     engineers may benefit from massively recorded real-world data in uncontrolled conditions,

389     which may leverage their design method. Indeed, engineers may focus most of their efforts on

390     optimising the most frequently used components; or they may extract the most relevant duty-

391     cycle from a large dataset of real-world data (Bishop et al., 2012). The dynamic characteristics

392     of front axle and cabin suspensions could be optimised in order to achieve the best balance

393     between on and off-road performance based on the frequency of each moving state and of the

394     most frequent operating speeds. Future work should focus on defining work states in greater

395     details and adapting the classification scheme in order to analyse real-time CAN-BUS data. In

396     this way, the algorithm could be embedded in in-vehicle computer systems and thus vehicle

397     sub-systems could be controlled based on the actual work state. For example, parameters of

398     tractor subsystems could be preventively set when the tractor is approaching a specific road

399     type (i.e. on-road or off-road), and that could be especially useful for setting the damping

400     coefficient of semi-active suspensions or the tyre pressure if the tractor embeds central tyre

401     inflating system.

**References**

ASAE. (2011). *ASAE D497.7—Agricultural Machinery Management Data* (D497.7; ASAE Standard, pagg. 1–15). https://doi.org/10.13031/2013.36431

Balsari, P., Biglia, A., Comba, L., Alcatrão, L., Varani, M., Mattetti, M., Barge, P., Tortia, C., Manzone, M., Gay, P., & Ricauda Aimonino, D. (2020). Performance analysis of a tractor—Power harrow system under different working conditions. *Soil and Tillage Research*. https://doi.org/Submitted

Bishop, J. D. K., Axon, C. J., & McCulloch, M. D. (2012). A robust, data-driven methodology for real-world driving cycle development. *Transportation Research Part D: Transport and Environment*, *17*(5), 389–397. https://doi.org/10.1016/j.trd.2012.03.003

Calcante, A., & Mazzetto, F. (2014). Design, development and evaluation of a wireless system for the automatic identification of implements. *Computers and Electronics in Agriculture*, *101*, 118–127. https://doi.org/10.1016/j.compag.2013.12.010

*Dati preconfezionati—GeoER*. (2019). http://geoportale.regione.emilia-romagna.it/it/download/dati-e-prodotti-cartografici-preconfezionati/pianificazione-e-catasto/uso-del-suolo-1/2014-coperture-vettoriali-uso-del-suolo-di-dettaglio-edizione-2018/dati-preconfezionati

Ettl, J., Bernhardt, H., Pickel, P., Remmele, E., Thuneke, K., & Emberger, P. (2018). Transfer of agricultural work operation profiles to a tractor test stand for exhaust emission evaluation. *Biosystems Engineering*, *176*, 185–197. https://doi.org/10.1016/j.biosystemseng.2018.10.016

Fugiglando, U., Massaro, E., Santi, P., Milardo, S., Abida, K., Stahlmann, R., Netter, F., & Ratti, C. (2019). Driving Behavior Analysis through CAN Bus Data in an Uncontrolled Environment. *IEEE Transactions on Intelligent Transportation Systems*, *20*(2), 737–748. https://doi.org/10.1109/TITS.2018.2836308

Harmon, J. D., Luck, B. D., Shinners, K. J., Anex, R. P., & Drewry, J. L. (2018). Time-Motion Analysis of Forage Harvest: A Case Study. *Transactions of the ASABE*, *61*(2), 483–491. https://doi.org/10.13031/trans.12484

Hodge, V. J., & Austin, J. (2004). A Survey of Outlier Detection Methodologies. *Artificial Intelligence Review*, *22*(2), 85–126. https://doi.org/10.1007/s10462-004-4304-y

Hunt, D., & Wilson, D. (2015). *Farm Power and Machinery Management: Eleventh Edition*. Waveland Press.

438 ISO. (2012). *ISO 11783-7:2012—Tractors and machinery for agriculture and forestry—Serial*
439 *control and communications data network—Part7: Implement messages application layer—*
440 *Implement messages application layer*.

441 Johannesson, P., & Speckert, M. (2013). *Guide to Load Analysis for Durability in Vehicle*
442 *Engineering*. John Wiley & Sons.

443 Kortenbruck, D., Griepentrog, H. W., & Paraforos, D. S. (2017). Machine operation profiles
444 generated from ISO 11783 communication data. *Computers and Electronics in Agriculture*,
445 *140*, 227–236. https://doi.org/10.1016/j.compag.2017.05.039

446 Lovarelli, D., Bacenetti, J., & Fiala, M. (2017). Effect of local conditions and machinery
447 characteristics on the environmental impacts of primary soil tillage. *Journal of Cleaner*
448 *Production*, *140*, 479–491. https://doi.org/10.1016/j.jclepro.2016.02.011

449 Marchesani, C., Parmigiani, F., & Vianello, M. (1992). *Integrated method to define the mission*
450 *profile of a passenger car*. Innovation and reliability in automotive design and testing,
451 Florence (I).

452 Mattetti, M., Maraldi, M., Sedoni, E., & Molari, G. (2019). Optimal criteria for durability test
453 of stepped transmissions of agricultural tractors. *Biosystems Engineering*, *178*, 145–155.
454 https://doi.org/10.1016/j.biosystemseng.2018.11.014

455 Mattetti, M., Molari, G., & Sedoni, E. (2012). Methodology for the realisation of accelerated
456 structural tests on tractors. *Biosystems Engineering*, *113*(3), 266–271.
457 https://doi.org/10.1016/j.biosystemseng.2012.08.008

458 Mattetti, M., Molari, G., & Sereni, E. (2017). Damage evaluation of driving events for
459 agricultural tractors. *Computers and Electronics in Agriculture*, *135*, 328–337.
460 https://doi.org/10.1016/j.compag.2017.01.018

461 Mattetti, M., Varani, M., Molari, G., & Morelli, F. (2017). Influence of the speed on soil-
462 pressure over a plough. *Biosystems Engineering*, *156*, 136–147.
463 https://doi.org/10.1016/j.biosystemseng.2017.01.009

464 Molari, G., Mattetti, M., Lenzini, N., & Fiorati, S. (2019). An updated methodology to analyse
465 the idling of agricultural tractors. *Biosystems Engineering*, *187*, 160–170.
466 https://doi.org/10.1016/j.biosystemseng.2019.09.001

467 Molari, G., Mattetti, M., Perozzi, D., & Sereni, E. (2013). Monitoring of the tractor working
468 parameters from the CAN-Bus. *AIIA 13*. Horizons in agricultural, forestry and biosystems
469 engineering, Viterbo.

470 Paraforos, D. S., Hübner, R., & Griepentrog, H. W. (2018). Automatic determination of
471 headland turning from auto-steering position data for minimising the infield non-working
472 time. *Computers and Electronics in Agriculture*, *152*, 393–400.
473 https://doi.org/10.1016/j.compag.2018.07.035

474 Paraforos, D. S., Vassiliadis, V., Kortenbruck, D., Stamkopoulos, K., Ziogas, V., Sapounas, A.,
475 & Griepentrog, H. W. (2017). Automating the process of importing data into an FMIS using
476 information from tractor's CAN-Bus communication. *Advances in Animal Biosciences*, *8*,
477 650–655. https://doi.org/10.1017/S2040470017000395

478 Perozzi, D., Mattetti, M., Molari, G., & Sereni, E. (2016). Methodology to analyse farm tractor
479 idling time. *Biosystems Engineering*, *148*, 81–89.
480 https://doi.org/10.1016/j.biosystemseng.2016.05.007

481  Pitla, S. K., Lin, N., Shearer, S. A., & Luck, J. D. (2014). Use of Controller Area Network
482  (CAN) Data To Determine Field Efficiencies of Agricultural Machinery. *Applied*
483  *Engineering in Agriculture*, *30*(6), 829–839. https://doi.org/10.13031/aea.30.10618

484  Pitla, S. K., Luck, J. D., Werner, J., Lin, N., & Shearer, S. A. (2016). In-field fuel use and load
485  states of agricultural field machinery. *Computers and Electronics in Agriculture*, *121*, 290–
486  300. https://doi.org/10.1016/j.compag.2015.12.023

487  Plaskitt, R. J., & Musiol, C. J. M. (2002). *Developing a Durable Product*. 1–20.

488  SAE. (2006). *Agricultural and Forestry Off-Road Machinery Control and Communication*
489  *Network* (N. j1939-2). https://saemobilus.sae.org/content/j1939/2_200608

490  SAE. (2013). *Vehicle Application Layer* (N. j1939-71; pagg. 1–1255).

491  SAE. (2016a). *SAE J1939-14—Physical Layer, 500 Kbps* (SAE J1939-14; pagg. 1–13).

492  SAE. (2018b). *SAE J1939-15—Physical Layer, 250 Kbps* (SAE J1939-15; pagg. 1–20).

493  Sehab, R., Barbedette, B., & Chauvin, M. (2011). Electric vehicle drivetrain: Sizing and
494  validation using general and particular mission profiles. *2011 IEEE International*
495  *Conference on Mechatronics*, 77–83. https://doi.org/10.1109/ICMECH.2011.5971228

496  Wong, J. Y. (2001). *Theory of Ground Vehicles*. John Wiley & Sons.

497  Zhang, Y., Ault, A., Krogmeier, J. V., & Buckmaster, D. (2017). Activity Recognition for
498  Harvesting via GPS Tracks. *2017 ASABE Annual International Meeting*.
499  https://doi.org/10.13031/aim.201700813

500